www.sciencemag.org/cgi/content/full/science.1190809/DC1

Supporting Online Material for

A Novel miRNA Processing Pathway Independent of Dicer Requires Argonaute2 Catalytic Activity

Daniel Cifuentes, Huiling Xue, David W. Taylor, Heather Patnode, Yuichiro Mishima, Sihem Cheloufi, Enbo Ma, Shrikant Mane, Gregory J. Hannon, Nathan D. Lawson, Scot A. Wolfe, Antonio J. Giraldez*

*To whom correspondence should be addressed. E-mail: antonio.giraldez@yale.edu

Published 6 May 2010 on *Science* Express
DOI: 10.1126/science.1190809

This PDF file includes:

Supplementary text for the main figures:

Figure 1: Analysis of MZdicer mutants revealed that not all miRNAs are affected to the same extent by the loss of Dicer function. One aspect worth noting is that due to the large fraction of small RNAs that correspond to miRNAs (~70-85%), some miRNAs might appear upregulated in *dicer*. It occurs because they are sequenced more often, probably due to the large depletion of other miRNAs that increase cloning efficiency of the remnant small RNAs. This does not necessarily mean they are upregulated in vivo, but rather that their overall representation in the sequenced small RNA population is increased due to the dramatic reduction other miRNA species. Thus, the results shown in the Fig. 1A, represent the relative dependence of each miRNA on Dicer for processing, rather than a direct measurement of the mature miRNA levels in the embryo. While we observe that several miRNAs appear to be processed in the absence of dicer. It is unclear whether they are processed by the same mechanisms operating on miR-451.

Figure 2: It has been shown that Ago 1-4 play redundant roles in miRNA mediated repression (*1*), however only Ago2 has slicer activity to cleave target mRNAs that are perfect complementary to the miRNA/siRNA loaded in RISC (*2, 3*). Our results indicate that wild type but not catalytic dead mutant Ago2 (D669A) restores mature miR-451 in vivo. Interestingly, miR-144, which is transcribed in

the same primary transcript than miR-451 and is co-expressed in the same cells, is largely unaffected by Ago2 loss of function (Fig 1B and C). These results suggest that while Ago2 can stabilize miRNAs, the loss of mature miR-451 is likely due to the catalytic processing of pre-miR-451 by Ago2 rather than destabilization due to loss of Ago2 function.

In vivo processing of miR-451 resulted in a weak broad band at ~30nt and a ladder between 22-26nt (Fig. 2F,). This miR-451 ladder, was reproducibly more intense in MZ*dicer* compared to wild type embryos and was consistent with the increase in the number of reads of 24-26bp (Fig. 1D). The higher levels of "free" Ago protein available in MZdicer mutants due to the overall reduction in mature miRNAs might account for the higher stability of these intermediate products during putative nucleolytic trimming *in vivo*. Alternatively, Dicer might play a role in the recruitment of the proposed exonuclease, increasing the half live of these intermediate products *in vivo*.

Supplementary discussion:

The identification of a miRNA-processing pathway that bypasses Dicer function might play a role in the processing of canonical miRNAs. It is worth noting that while we identify an Ago2-dependent, Dicer-independent mechanism responsible for processing miR-451 *in vivo*, it is unclear whether the same mechanisms are responsible for the refractory behavior of other miRNAs to Dicer loss-of-function. Indeed, according to the results shown in Fig. 1B, Ago2 does not appear to be strictly required to process mature miR-735-5', -146-5', and -2190, and future studies will be required to elucidate how these miRNAs are processed in vivo. Interestingly, two different laboratories have reported that some miRNAs are still present in dicer-/- ES cells, albeit at 10 to 100-fold reduced levels compared to wild type cells (*4, 5*). Future studies will be required to determine whether some miRNAs that are preferentially processed by Dicer, can also be processed by Ago2 cleavage of the passenger strand in the pre-miRNAs and

bypass Dicer function *in vivo.* This might explain the different requirements for Dicer on different miRNAs observed in this (Fig. 1A) and other studies (*4, 5*).

In plants, the slicer activity of Ago2 has been shown to cleave endogenous mRNAs that possess target sequences displaying perfect complementarity to siRNA guides (*6, 7*). However, in animals, few targets exhibiting perfect complementary to miRNAs have been found (*7, 8*), implying that Ago2's physiological function in animals might use a mechanism other than direct cleavage of mRNA targets. Loss of Ago2 activity in mice results in early embryonic lethality (*2*), in part due to defects within the placenta (*9*). In zebrafish, some zygotic *ago2* mutant embryos survive to adulthood due in part to maternally provided Ago2 activity, allowing the generation of maternal-zygotic *ago2* mutants. Interestingly, we find that Ago2 is strongly expressed in developing blood cells, where it has been previously shown to have slicer-independent roles (*10*). Specifically, loss of Ago2 function results in failure to process miR-451, anemia and erythrocyte maturation defects. Providing back miR-451 or wild type Ago2 but not catalytically dead mutant, rescues the maturation defects. Our study provides a biological context in which Ago2 slicer activity is needed to process a blood-specific miRNA miR-451. While it is likely that Ago2 has additional roles in the cell, the strong conservation of the sequence and secondary structure of miR-451 across vertebrate species suggests that significant constraints have been in place to maintain the miRNA-processing activity of Ago2 through evolution.

Our results show that the secondary structure of a pre-miRNA hairpin determines whether it is processed via Dicer- or Ago2-mediated cleavage. While canonical Dicer-processed hairpins are typically 55-75 nt, miR-451 encodes a 42nt miRNA hairpin in which the mature miRNA extends into the loop region, with extensive complementary pairing within the central region of the stem. Other miRNAs with extensive pairing in the middle portion of the stem, corresponding with the slicer cleavage site could be processed by Ago2. The results presented

here demonstrate that a Dicer-dependent hairpin can be modified to take a Dicer-independent Ago2-dependent pathway by mimicking the secondary structure of miR-451 (Fig. 4). Future work will be geared toward identifying additional endogenous hairpin sequences that might potentially serve as substrates for Ago2-mediated processing.

These results have several implications for small RNA applications in research and therapy. The adoption of Ago-dependent hairpin structures in the delivery of exogenous siRNAs might improve processing efficiency and activity by ensuring that the guide strand is preferentially incorporated into Ago2. In addition, the findings presented here provide a means to genetically express microRNAs in a dicer-null background, to dissect the functions of individual miRNAs.

In summary, the study of miR-451 and its processing by Ago2 reveals a novel miRNA-processing pathway that functions independently of the central RNaseIII enzyme Dicer, and provides an entry point to uncover novel small regulatory RNAs that use this processing pathway.

Figure legends:

Fig. S1: Characterization of microRNAs in MZ*dicer* and MZago2 mutants (A) Schematic representation of Dicer domains and the positions of the point mutations. Both mutant alleles induce a premature stop codon. *dicer*^{hu715} encodes a mutation E1416X that results in a predicted truncation that lacks the RNaseIII and the dsRNABD. *dicer*^{hu896} Y172X encodes a protein with a predicted N-terminal truncation that lacks the HelicaseC, PAZ, RNaseIII and dsRNABD. Positions of the point mutations are given according to the predicted start site of the mRNA. (B) Sequence conservation for the miR-451 loci in human (hsa),

mouse (mmu), frog (xtr) and zebrafish (dre). (C) Graphical representation of the genomic sequence encoding the first 31 nt of miR-451 and the reads that map miR-451 (lower graph). Note that the most frequent base after nt 30 is a non-templated uridine. (D) Working model derived from the read analysis suggests that (i) the pre-miR-451 is cleaved in the miRNA* sequence 10 nt from the 5'end of the mature miRNA by Ago2, (ii) this product is polyuridylated, and (iii) trimmed to form the mature, functional miRNA. (E) Schematic representation of the Zinc Finger Nuclease (ZFN) consisting of two zinc finger proteins (ZFP) fused to a FokI nuclease domain and bound to the target in exon 14 of the *ago2* gene (*11-13*). Sequences of zinc finger recognition helices and the triplet DNA target sequences are shown on the left. (F) Genomic sequence of the ZFN-induced double-strand break in the mutant *ago2Δ90*. This lesion removes 90nt in exon 14 including a splice-donor site causing an out-of-frame deletion within the region coding the Piwi domain of Ago2 at nt 1847 that removed a splice-donor site (*ago2*^{yD90}). This allele encodes a predicted truncated Ago2 protein that lacks part of the Piwi domain, including two of the three catalytic sites (Fig. 1E) Schematic representation of the slicer cleavage assay shown in figure 1F: Northern blot of embryos to detect an injected GFP target mRNA with three perfectly complementary targets to miR-1 (3xPT-miR-1) in wild type, MZ*ago2 or Zago2* embryos in the presence (+) or absence (–) of miR-1 (*14, 15*). (H) Northern blot to assay slicer activity in zygotic Ago2 mutants. Early in development zygotic mutants are indistinguishable from heterozygous embryos. Thus, to test whether slicer activity is reduced in Zago2 mutants we analyzed slicer cleavage in wild-type embryos and Zago2-/? mutants, where ! of the embryos where -/- and ! were -/+. We did not observe a significant reduction in slicer activity in Zago2 -/? mutant embryos compared to wild type, suggesting that there is a significant maternal contribution for Ago2 slicer function.

Fig. S2 (Table S1): Summary of small RNA mapping to the Zebrafish genome in WT, MZ*dicer*$_{hu715}$, MZ*dicer*$_{hu896}$ and MZ*ago2*$_{y^{n}\ 90}$.

Fig. S3: Scatter plot of each individual miRNA from *dicer*$_{hu715}$ vs. wild type at 48 hours. Expression level of each miRNA was normalized to the total number of reads mapped to the genome in wild type and *dicer*$_{hu71}$, respectively.

Fig. S4: Scatter plot of each individual miRNA in *dicer*$_{hu896}$ vs. wild type at 48 hours. Expression level of each miRNA was normalized to the total number of reads mapped to the genome in wild type and *dicer*$_{hu896}$, respectively.

Fig. S5: Conservation of miR-451 hairpin structure across 13 species. Mature miRNA sequence is labeled in red for each hairpin structure.

Fig. S6: *In situ* hybridization for ago1, 2, 3, and 4 in wild type zebrafish embryos. (A) Whole-mount *in situ* hybridization of Ago1-4 at one cell stage and 24hpf. Ago1-4 are maternally provided but acquire tissue specific expression by 24hpf. **(B)** Fluorescent micrograph of wild type or MZ*ago2* mutant embryos injected with GFP-miR-1 reporter and a control dsRed mRNA at 9hpf. The GFP miR-1 reporter has three partially complementary sites to miR-1 (GFP- 3xIPT). GFP expression is shown in green and dsRed is shown in red. GFP reporter expression is repressed when a miR-1 duplex is injected in either wild type or MZ*ago2* mutant embryos. These results suggest that despite the strongly reduced slicer-mediated mRNA cleavage (Fig. 1F) in MZago2 mutants, in the early embryo, Ago function during miRNA mediated repression is likely compensated at least in part by maternally provided Ago1, 3 or 4. These results are consistent with previous reports indicating redundant functions of Ago-1-4 for miRNA-mediated repression in mammalian cells (*1*).

Fig. S7: Electrophoretic mobility shift assay with Dicer protein, miR-451 and miR-430 hairpins. EMSA using excess 5' ^{32}P-labeled pre-miR-451, pre-miR-430c or a miR-451 hairpin with mismatches in positions 10 and 11 (mm10-11) and recombinant human Ago2 (hAgo2, A, B) or recombinant human Dicer (hDicer, +)(B). Binding was reduced when an unlabeled pre-miRNA competitor was added (+), while non-specific competitor (tRNA, lanes 1, 2, or GFPmRNA lane 4, panel A) did not reduce binding. See material and methods for details.

Fig. S8: Morphogenesis in MZ*ago2* mutants compared to wild type and MZ*dicer* mutants. Compared to wild type embryos (A), MZ*ago2* mutants (B) do not show morphological defects at ~32hpf. This is in contrast to MZ*dicer* mutant embryos (C) that show defects during gastrulation, brain morphogenesis, trunk and heart development (*14*). Lower panels show dorsal and lateral view of the head region. Arrows denote the brain ventricles (red) and the mid-hindbrain boundary (MHB, yellow). Note the normal formation of the brain ventricles and the MHB in MZ*ago2* compared to MZ*dicer* mutants. (D) Diagram representing the areas shown in the panels (E, dotted box). (E) Expression of hemoglobin (brown) visualized by the oxidation of o-dianisidine at 48hpf. (C) Lateral view of the zebrafish tail in different genotypes as indicated. Hemoglobinized cells, labeled by o-dianisidine staining, accumulate in the caudal vein and the aorta of wild type and MZ*dicer* mutants but are reduced in MZ*ago2* mutants. Others and we have used *dicer* mutants to evaluate the global function of miRNAs (*14, 16-21*). Such analyses provide an important start point to understand the function of Dicer dependent small RNAs. Indeed, loss of Ago2 function (Fig. 3) and knock down of miR-451 (*22*) both result in erythrocyte maturation defects that are not observed in MZ*dicer* mutants. The identification of Dicer-independent miRNA processing highlights the importance of functional analysis of individual miRNA families to uncover their role in vivo.

Fig. S9: *In situ* hybridization for hematopoietic markers in wild type and MZ*ago2* embryos. Primitive progenitor cells, erythrocytes, and myeloid cells labeled by whole mount in situ hybridization with Gata2, Hemoglobin beta embryonic 3 (Bglobin3), and lymphocyte cytosolic plastin 1 (lcp1) RNA probes, respectively. Embryos were collected at 20 somites (gata2), 24 hpf (Bglobin3) and 30hpf (lcp1). Consistent with the reported expression of miR-451 in erythrocytes, analysis of other hematopoietic markers (*23*) such as scl, gata2 (primitive progenitor cells), and lymphocyte cytosolic plastin 1 (lcp1, myeloid marker) did not reveal major differences between wild type and MZ*ago2* mutant embryos.

Fig. S10: miR-1 ago hairpin regulates a GFP miR-1 reporter. (A) Northern blot to detect *in vivo* processing of a synthetic miR-1-ago hairpin with the secondary structure of pre-miR-451. (B) Fluorescent micrograph of embryos injected with GFP-miR-1 reporter and a control dsRed mRNA at 9hpf. The GFP miR-1 reporter has three partially complementary sites to miR-1 (GFP- 3xIPT). GFP expression is shown in green and dsRed is shown in red. GFP reporter expression is repressed when a miR-1 duplex or a miR-1$^{ago\text{-}hairpin}$ are injected at one cell stage. The sequence of the miR-1 duplex and the miR-1$^{ago\text{-}hairpin}$ with the secondary structure of miR-451 are shown below. The mature miRNA is shown in red.

Fig. S11: Model of Ago2-mediated miRNA processing. Dicer-independent pathway for miRNA processing that is dependent on Ago2 catalytic activity. We propose the following step-wise model for Ago-mediated miRNA processing: (i) binding of Ago2 to a pre-miRNA hairpin, (ii) Ago2-mediated cleavage of the paired miRNA* passenger strand at a position +10 nts relative to the 5'end of the Ago2-bound miRNA guide strand, (iii) based on the small RNA sequences of miR-451 we favor a model where the cleaved precursor is polyuridylated at the cleavage site, and (iv) nuclease-mediated removal of uridines and templated nucleotides not protected by Ago2 then generate the mature miRNA.

Materials and Methods

Zebrafish strains

MZ*dicer* mutant embryos (*dicer*^{hu896} and *dicer*^{hu715}) were generated by germline replacement as described previously (*14*). *dicer*^{hu715} encodes a mutation E1416X that results in a predicted truncation that lacks the RNaseIII and the dsRNABD). *dicer*^{hu896} Y172X encodes a protein with a predicted N-terminal truncation that lacks the HelicaseC, PAZ, RNAseIII and dsRNABD. Ago2 mutants were generated by gene targeting using zinc finger nucleases (See below) (*13*) (*11*). We generated maternal and zygotic *ago2* (MZ*ago2*) mutant

embryos by incrossing *ago2*-/- adults and selecting for homozygous mutant escapers.

Modular ZFN assembly

Two ZFN with three zinc finger modules each were designed and assembled to target a region in exon 14 of argonaute2 within the PIWI domain (Fig 1E). The resulting ZFN pair recognize the target sequence 5'ACTCATCCACCAGCTGGAGATGGCA3'. Individual zinc finger modules based on Zif268 backbone were individually amplified by PCR from an archive of modules constructed for this purpose (Smith, Zhu, Rayla, McNulty, Lawson and Wolfe, *unpublished results*). Each individual ZFP was PCR-amplified using the appropriate primer set (F1, Finger 1; F2, Finger 2, and F3, Finger 3) and purified.

F1 forward: 5'-GCGATGGGTACCCGCCCATATGCTTGCCC

F1 reverse: 5'-CACTGGAAGGGCTTCTGGCCTGTGTGAATCCGGATGTG

F2 forward: 5'-CATCCGGATTCACACAGGCCAGAAGCCCTTCCAGTGTCGCATCTGC F2 reverse: 5'-ATGTCGCATGCAAAAGGCTTCTCGCCTGTGTGGGTGCGGATGTG

F3 forward: 5'-CAGGCGAGAAGCCTTTTGCATGCGA

F3 reverse: 5'-GCGTAGGATCCACCTGTGTGGATCTTGGTGTG

The F1 reverse/F2 forward and F2 reverse/F3 forward primers contain complementary sequences that allow overlapping PCR amplification to generate a single contiguous fragment containing all three fingers. 30 mg of purified PCR product for each finger was combined in a single PCR reaction to assemble the three-finger cassette and amplified using the F1 forward and F3 reverse primers. This PCR product was digested with KpnI and BamHI and was cloned into a pCS2-based expression vector for generating ZFN-encoding mRNAs for injection into zebrafish embryos (*13*). Each construct contained the DD (D483R) or RR (R487D) engineered variants of the FokI nuclease domain (*24*) bearing a TGGS linker between the ZFP and nuclease domain.

5’ ZFP sequence (KpnI/BamHI):
GTRPYACPVESCDRRFSRSDNLTRHIRIHTGQKPFQCRICMRNFSLSFNLTRHI
RTHTGEKPFACDICGRKFARSDALTRHTKIHTGGS

3’ ZFP sequence (KpnI/BamHI):
GTRPYACPVESCDRRFSEKSHLTRHIRIHTGQKPFQCRICMRNFSLSFNLTRHI
RTHTGEKPFACDICGRKFAQRGHLTRHTKIHTGGS

Generation and screening of MZ*ago2* mutant fish strain

50 pg of each 5’ and 3’ ZFN mRNA was injected into wild type embryos (F0) at the one-cell stage and embryo morphology was scored at 24 hpf. At least half of the injected embryos showed severe developmental defects at this dose, indicating that the ZFN is active. The morphologically normal embryos were raised to adulthood and intercrossed to produce F1 embryos. These embryos were genotyped in order to identify the parental founder mutants. Genotyping was conducted as follows: 30 embryos from each pair were sorted into 6 groups of 5 embryos each and placed into PCR tubes with 150 µl of 100 mM NaOH. The embryos were boiled for 20 minutes at 95C. This crude genomic DNA extract was neutralized with 20 µl of 1 M Tris-HCl pH 7.4 (Sigma) and 5 ul of the extract were used directly as a template for the genotyping PCR. 1 µl of the PCR product was diluted in 14 µl of formamide and submitted for fragment analysis at DNA Analysis Facility (Yale University). The chromatograms were analyzed with the GeneMapper software for extra chromatogram peaks apart from wild type that would indicate the presence of an insertion/deletion in the loci. The identified mosaic founder F0 mutants were backcrossed to wild type with the purpose of raising a heterozygous F1 and diluting possible off-target mutations. F2 families of heterozygous carriers derived from individual founders were used to generate zygotic *ago2* (Z*ago2*) mutant embryos that still maintained slicer activity at initial stages of development due to maternal contribution (fig. S1). Some homozygous mutant embryos survived to adulthood and were incrossed to generate zygotic *ago2* (MZ*ago2*) mutant.

Computational methods.

Small RNA sequence reads were generated from the Illumina analysis pipeline. In the assessments of wild-type samples, we found 871,098 and 2,276,394 genome-matching sequence reads. The MZ*dicer* $^{hu715/hu715}$ and MZ*dicer* $^{hu896/hu896}$ mutants gave 2,264,413 and 2,493,924 reads, respectively. MZago2 mutant sample gave a total of 15,900,662 genome-matching reads. The low complexity reads (e.g. single nucleotide repeats of more than 30 nt in length) were filtered out and 3' adapter sequences were trimmed using the R ShortRead package. The trimmed reads were then mapped to the zebrafish reference genome (Ensembl Zv8) using the Bowtie alignment algorithm (version 0.12.1) with an allowance for 2 mismatches within the first 20 nt. The best matched reads with no more than 200 mapping locations in the Zv8 genome were kept for further analysis. All 5' and 3' derived miRNAs were inferred based on the most abundant reads that aligned to the stem region of known miRNA precursor sequences. Only those reads that aligned with the exact start site of mature miRNAs and were greater than 20 nucleotides in length were counted. The count value for each mature miRNA was normalized to the total number of reads that mapped to the Zv8 genome and multiplied by 1,000,000. Reads that aligned to multiple locations in the genome were scaled to unique mapping reads. Pre-miRNA length was measured starting from the first nt of the 5' end miRNA and ending 2-nt beyond the last nt of the 3' end miRNA sequence (instead of miRbase annotated full-length precursor sequences).

miRNA duplexes, mRNA synthesis and injection

mRNA for injection was transcribed using the SP6 mMessage mMachine kit according to the manufacturer's instructions (Ambion). 1000 pl of a 0.2 µg/µl mRNA solution encoding for FLAG-mouse Ago2 was injected into wild-type, MZ*dicer* or *MZago2* embryos at the one-cell stage. Injected mRNAs to express Ago2 encoded for Flag-mouse Ago2. The miRNA hairpins and duplexes were purchased from IDT or Dharmacon and resuspended in the manufacturer's buffer

to a concentration of 1 mM. Working aliquots were prepared in RNase free water at 50 µM and stored at –80C. miRNA:miRNA* and hairpin sequences are shown below. 1000pl of a 50µM solution were injected per embryo for miRNA duplexes and hairpins.

>1249: pre-miR-451
5'rArArArCrCrGrUrUrArCrCrArUrUrArCrUrGrArGrUrUrUrArGrUrArArUrGrGrUrArArGrGrGrUrUrCrUrG3'

>1250: pre-miR-451-mm10-11
5'ArArArCrCrGrUrUrArCrCrArUrUrArCrUrGrArGrUrUrUrArGrUrArArUrCrCrUrArArGrGrGrUrUrCrUrG3'

>1252: miR-451 duplex
5'ArArArCrCrGrUrUrArCrCrArUrUrArCrUrGrArGdTdT3'
5'CrUrCrArGrUrArArUrGrGrUrArArCrGrGrUrArUdTdT3'

>miR-451 LNA probe
5'AACTCAGTAATGGTAACGGTTT3'

>1253: pre-miR-430c (Ago hairpin)
5'rUrArArGrUrGrCrUrUrCrUrCrUrUrUrGrGrGrGrUrGrUrUrCrCrArArArGrArGrArArGrGrArCrUrUrCrUrC3'

>1264 miR-430c (Dicer hairpin)
5'rUrArArGrUrGrCrUrArUrUrUrUrGrUrUrGrGrGrGrUrArUrArArGrArUrUrCrUrArArArArUrUrArArGrCrCrUrCrArArCrArArArUrArGrGrArUrUrUrGrArA3'

Rescue of the MZago2 embryos (Fig 3) was performed by injecting 1000pl of a 0.05 µg/µl of wild type or catalytically dead (D669A) FLAG-mouse Ago2 (*10*)

mRNA or 50 µM solution of miR-451 duplex (*22*)

5′ end labeling of oligonucleotides

RNA hairpins, DNA oligonucleotides, and LNA probes were 5' end-labeled using T4 polynucleotide kinase (PNK, New England Biolabs) in 20 µl reactions containing 50 µM of oligonulceotide, 1# PNK buffer and 50 µCi of $-^{32}P-ATP at 37 °C for 60 min and unincorporated nucleotides were removed using illustra^{TM} Microspin G-50 columns. Labeled RNA hairpins used for *in vitro* cleavage assays where further PAGE purified. Briefly, the RNA hairpins were eluted from the gel slices by soaking overnight in 300 µl of 0.4 M of NaCl followed by standard ethanol precipitation.

Northern blot

To detect endogenous microRNAs, a total of 20-30 embryos were collected at the indicated time points and flash frozen in liquid nitrogen. Total RNA was extracted using Trizol (Invitrogen) and resuspended in formamide. Loading buffer 2x (8 M urea, 50 mM EDTA, 0.2 mg/ml bromophenol blue, 0.2 mg/ml xylene cyanol) was added and the samples were boiled for 5 minutes at 95°C. The samples were separated by electrophoresis using denaturing 15% polyacrilamide gels in 1x TBE buffer. The gel was transferred to a Zeta-Probe Blotting membrane (BioRad) using a semi-dry Trans-Blot SD (BioRad) at 20 V (0.68 A) for 35min. RNA was crosslinked to the membranes by UV exposure at 1200 µJ/cm^2. Membranes were pre-hybridized with 15 ml of ExpressHyb Hybridization Solution (Clontech) for 1 h at 50°C with constant rotation. 3,000,000 cpm of 5' $ -^{32}P labeled probe was added to 15 ml of ExpressHyb and incubated overnight at 45°C for LNA probes (Exiqon) and at 30°C for DNA oligonucleotide probes. DNA oligonucleotides were labeled using the StarFire method (IDT) using alpha α-^{32}P-dATP to increase sensitivity. Membranes with LNA were washed twice at 50°C with 5x SSC/10% SDS for 10 minutes and once for 10 minutes with 1x SCC/1% SDS. Membranes hybridized with oligonucleotide DNA probes where washed at room temperature with 2x SSC/0.1% SDS

followed by 1x SSC/0.1% SDS for 15 minutes. Northerns in Figure 2A, D, E, F where hybridized with miR-451 LNA probe. Northerns in Figures 2F and Figure 4C were hybridized with miR-430a LNA probe. Northern in fig. S10 was hybridized with miR-1 StarFire probe.

Electrophoretic Mobility Shift Assay

To test the hairpin-binding activity of Ago2, 10 μM of 5'-labeled hairpin and 5 μM hAgo2 were incubated in a 10 μl reaction volume containing 20 mM HEPES- HCl, pH 7.5, 150 mM KCl, with a specific cold competitor (miRNA hairpin 200 μM) or an unspecific cold competitor (tRNA or GFP mRNA), at 23 °C for 10 minutes The reaction products were separated by 8% native PAGE at 160 V for 60 minutes at 4°C. To determine if these same hairpins bind to Dicer, 5 μM of 5'-labeled hairpin and 2 μM hDicer were incubated in a 10 μl reaction containing 20 mM HEPES, pH 7.5, 150 mM KCl, 3 mM EDTA, with and without 200 μM of specific cold competitor, at 0°C for 30 minutes. The reaction products were separated by 4.5% native PAGE at 120 V for 75 minutes at 4°C. The gels were quantified by Phosphorimager analysis.

Ago2 and Dicer *in vitro* cleavage Assays

To test the ability of recombinant Ago2 to process the hairpin substrates, a slicer cleavage assay was performed as described previously (*25*). Briefly, 5 μM of PAGE-purified 5'-labled hairpin and 1 μM hAgo2 were incubated in a 10 μl reaction volume containing 3 μg of yeast tRNAs, 25 mM HEPES-KOH, pH 7.5, 50 mM potassium acetate, 5 mM magnesium acetate and 5 mM DTT at 37°C for 4 h. Reactions were stopped by adding equal volumes of phenol:chloroform:isoamy-alcohol, precipitating in ethanol and separating the resuspension by 15% PAGE with 7 M urea. The gel was blotted onto a nitrocellulose membrane and quantified by Phosphorimager analysis. To test the ability of recombinant Dicer to process the same substrates, a dicing assay was performed as described previously (*26*). Briefly, 5 μM of PAGE-purified 5'-labeled hairpin and 120 nM hDicer were incubated in a 10 μl reaction volume

containing 20 mM Tris-HCl, pH 6.5, 1.5 mM $MgCl_2$, 25 mM NaCl, 1 mM DTT, and 1% glycerol at 37°C for 60 min. Reactions were stopped by adding 1 volume of loading buffer (8 M urea, 50 mM EDTA, 0.2 mg/ml bromophenol blue, 0.2 mg/ml xylene cyanol and heating at 95 °C for 10 min. The reaction products were analyzed by 15% PAGE with 7M urea and quantified by Phosphorimager analysis.

RNase protection assay

For the RNase protection assay, Ago2 cleavage reactions were performed as described previously, followed by the addition of 1,000 units of RNase I (Ambion) for 30 minutes at 23˚C. The reactions were stopped by the addition of 1 µl of 20mg/ml Proteinase K (Ambion) for 30 minutes at 37˚C. Reaction products were separated by 15% PAGE with 7 M urea and quantified by Phosphorimager analysis

***In situ* hybridization of Ago and WT zebrafish embryos**

Plasmids to transcribe *in situ* probes for blood markers were kindly provided by Scott Lacadie and Leonard Zon. Probes for argonaute paralogs were amplified from 0hpf cDNA and cloned BamHI-XhoI in pBluescript. Sequences of oligo pairs (top/bottom) used were:
Ago1 (5'caaggatccCGCCCCTGCAGCAGGTGTTTCAGGCG3'/
5'caactcgagCATCAATGTTACGTATGTCCAGG3'),
Ago2 (5'caaggatccCACCACAAGAATATGTCTTCAAACCA3'/
5'caactcgagCTTCGATGCTTTTAAAATCCAAA3'),
Ago3 (5'caaggatccTTGGGGCTGCGCCCCAGTTCTCCGTA3'/
5'caactcgagCATCGATGTTGTGGATATCAAGA3'),
Ago4 (5'caaggatccCTGCCCCTACCTCCCTCTTCCAGCCA3/
5'caactcgagCGTTGATGTTCTGGATGTCCAAA3').
In vitro transcription of antisense digoxigenin (DIG) labeled RNA probes was performed in 20 µl reactions containing 4 µl 5X transcription buffer (Promega), 2 µl 100mM DTT (Promega), 2 µl DIG RNA labeling mix (Roche), 2 µl RNase free

H_20 (Ambion), 1 µl T7 RNA polymerase (Promega), 1µl RNase inhibitor (Roche) and 8 µl of linearized purified plasmid. Probes were purified using Illustra Microspin G-50 Columns (GE Healthcare). Embryos at various stages between 20 somites and prim 5 were fixed overnight at 4°C in 4% PFA (paraformaldehyde)/PBS, gradually dehydrated in methanol/PBS, and stored at -20°C in 100% methanol for at least 5 hrs. In situ hybridization was performed as described previously (*27*). Embryos were fixed in 4%PFA after staining, dehydrated in methanol and cleared in benzyl benzoate/benzyl alcohol before they were photographed.

Brain ventricle labeling using TxRed dextran.

24 hpf embryos were mounted in a thin layer of 0.4% low-melting agarose and 1000 pl of Texas Red dextran 70,000MW (1:20 dilution of a 500µg/µl stock, Molecular Probes) was injected into the brain ventricles as described in (*14, 28*).

Image acquisition

Embryos were analyzed using a Zeiss Axioimager M1 and Discovery microscopes and photographed with a Zeiss Axiocam digital camera. Images were processed with Zeiss AxioVision 3.0.6. For whole mounts, different focal planes were merged into a single image using Adobe Photoshop CS2 software.

FLAG-mAgo2 constructs

Mouse Ago2 WT and mutant were kindly provided by D. O'Carrol (*10*). The open reading frame of Ago2 WT and the mutant D669A plus the FLAG tag were amplified with oligos 1078a and 1078b and then cloned into pCS2+ using Clontech In-Fusion™ PCR Cloning System.

1078a 5'CCATCGATTCGAATTCATGGACTACAAGGACGATGACAAG3'

1078b 5'TCACTATAGTTCTAGATCAAGCAAAGTACATGGTGCG3'

FLAG-mAgo2 immunoprecipitation.

Embryos were injected with FLAG-mAgo2 WT and either miR-451 hairpin or miR-451 mm10-11. 100 embryos were collected 7 hr after injection from each sample and washed twice with PBS. The embryos were transferred to a new tube with 500 µl of NET-2 buffer (100 mM Tris-HCl pH 7.5, 150 mM NaCl, 0.05% NP-40) and 1 µl of RNase inhibitor (Roche). The embryos were sonicated for 3 cycles of 15 seconds followed by 15 seconds rest on ice. Lysates were cleared by centrifugation at 16,000 x g. 50 µl of supernatant was kept as input and the rest of the was added to 500 µl of NET-2 with 2.5 mg of protein A-sepharose that had been blocked with 50 µg of tRNA for 30 minutes at 4°C. 1 µl of a rabbit anti-FLAG antibody 1 µg/µl (Sigma) was added to the mixture and the samples were incubated overnight at 4°C with orbital shaking. 50 µl of supernatant was removed for further analysis. The beads were washed 4 times with 500 µl of NET-2 buffer at 200 x g for 3 minutes at 4°C. 500 µl of Trizol (Invitrogen) was added to the beads, and RNA was purified using standard techniques.

O-Dianisidine staining

O-dianisidine solution at 0.7 mg/ml was prepared fresh in ethanol and protected from exposure to light. The staining solution was prepared by mixing 2 ml of water, 2 ml of 0.7 mg/ml O-dianisidine, 0.5 ml of 100 mM sodium acetate, and 100 µl 30% hydrogen peroxide. PTU treated embryos were transferred to a 12-well plate and 1 ml of the staining solution was added. Stained embryos were kept in the dark for 15 minutes, washed three times with PBS, and finally fixed with 4% paraformaldehyde.

Evaluation of the anemic phenotype

After o-dianisidine staining at 48 h, MZ*ago2* embryos were sorted in three categories according to the amount of o-dianisidine positive cells: - *Group 1* (similar to wild type): embryos present an level of staining similar to wild type controls, with cells spreading all along the ducts of Cuvier and the heart. - *Group*

2 (intermediate): embryos in this category have o-dianisidine positive cells but individual cells are still visible. -*Group 3* (almost bloodless): these embryos have less than 100 o-dianisidine positive cells in the ventral and rostral area and no other major accumulation in the posterior blood island. Six independent crosses of MZago2 mutants were analyzed for o-dianisidine staining.

To evaluate the degree of erythrocyte maturation, groups of 20 zebrafish embryos were bleed at 60hpf in a glass slide and blood cells were prepared by cytospin as described in (*22*). Blood cells were stained with May-Grünwald/Giemsa solutions (Polysciences), imaged and photographed using a Zeiss Axioimager M1 microscope. The pixel area of the nucleus and cytoplasm was quantified for 50-150 cells per sample in three independent experiments using ImageJ software as described in (*22*) and the nuclear:cytoplamic ratio calculated for each cell. Statistical analysis of the different samples was done using a Wilcoxon rank-sum test, and the p-values were corrected for multiple testing (Bonferroni correction, 7 tests).

Slicer cleavage assay.

A GFP reporter mRNA with three perfect complementary sites to miR-1 in the 3'UTR (GFP-3xPT) (*14*) was injected at one cell stage (1000 pl of 0.2 µg/µl mRNA) with or without miR-1 duplex (*14*) (1000 pl of a 50 µM) in wild type and MZ*ago2* mutant embryos. Total RNA from 20 embryos was extracted at 3-4 hours after injection and the 5' fragment of GFP reporter mRNA was detected by Northern blot using a DNA probe complementary to the GFP sequence. The probe was labeled by random priming with α-^{32}P-dCTP using Megaprime DNA Labelling System (Amersham) according to manufacturer's instructions.

1. H. Su, M. I. Trombly, J. Chen, X. Wang, *Genes Dev* **23**, 304 (Feb 1, 2009).
2. J. Liu *et al.*, *Science* **305**, 1437 (Sep 3, 2004).
3. G. Meister *et al.*, *Mol Cell* **15**, 185 (Jul 23, 2004).
4. J. M. Calabrese, A. C. Seila, G. W. Yeo, P. A. Sharp, *Proc Natl Acad Sci U S A* **104**, 18097 (Nov 13, 2007).

5. J. E. Babiarz, J. G. Ruby, Y. Wang, D. P. Bartel, R. Blelloch, *Genes Dev* **22**, 2773 (Oct 15, 2008).
6. J. F. Palatnik *et al.*, *Nature* **425**, 257 (Sep 18, 2003).
7. D. P. Bartel, *Cell* **136**, 215 (Jan 23, 2009).
8. S. Yekta, I. H. Shih, D. P. Bartel, *Science* **304**, 594 (Apr 23, 2004).
9. S. Cheloufi, C. O. Dos Santos, M. M. W. Chong, G. J. Hannon, *Nature* (2010).
10. D. O'Carroll *et al.*, *Genes Dev* **21**, 1999 (Aug 15, 2007).
11. Y. Doyon *et al.*, *Nat Biotechnol* **26**, 702 (Jun, 2008).
12. M. L. Maeder *et al.*, *Mol Cell* **31**, 294 (Jul 25, 2008).
13. X. Meng, M. B. Noyes, L. J. Zhu, N. D. Lawson, S. A. Wolfe, *Nat Biotechnol* **26**, 695 (Jun, 2008).
14. A. J. Giraldez *et al.*, *Science* **308**, 833 (May 6, 2005).
15. A. J. Giraldez *et al.*, *Science* **312**, 75 (Apr 7, 2006).
16. C. M. Takacs, A. J. Giraldez, *Semin Cell Dev Biol* (Feb 10).
17. R. Yi *et al.*, *Nat Genet* **38**, 356 (Mar, 2006).
18. B. D. Harfe, M. T. McManus, J. H. Mansfield, E. Hornstein, C. J. Tabin, *Proc Natl Acad Sci U S A* **102**, 10898 (Aug 2, 2005).
19. E. Bernstein *et al.*, *Nat Genet* **35**, 215 (Nov, 2003).
20. E. P. Murchison *et al.*, *Genes Dev* **21**, 682 (Mar 15, 2007).
21. T. Andl *et al.*, *Curr Biol* **16**, 1041 (May 23, 2006).
22. L. Pase *et al.*, *Blood* **113**, 1794 (Feb 19, 2009).
23. J. L. de Jong, L. I. Zon, *Annu Rev Genet* **39**, 481 (2005).
24. M. Szczepek *et al.*, *Nat Biotechnol* **25**, 786 (Jul, 2007).
25. B. Wang *et al.*, *Nat Struct Mol Biol* **16**, 1259 (Dec, 2009).
26. E. Ma, I. J. MacRae, J. F. Kirsch, J. A. Doudna, *J Mol Biol* **380**, 237 (Jun 27, 2008).
27. C. Thisse, B. Thisse, T. F. Schilling, J. H. Postlethwait, *Development* **119**, 1203 (Dec, 1993).
28. J. H. Gutzman, H. Sive, *J Vis Exp* (2009).

fig. S1 Cifuentes et al.

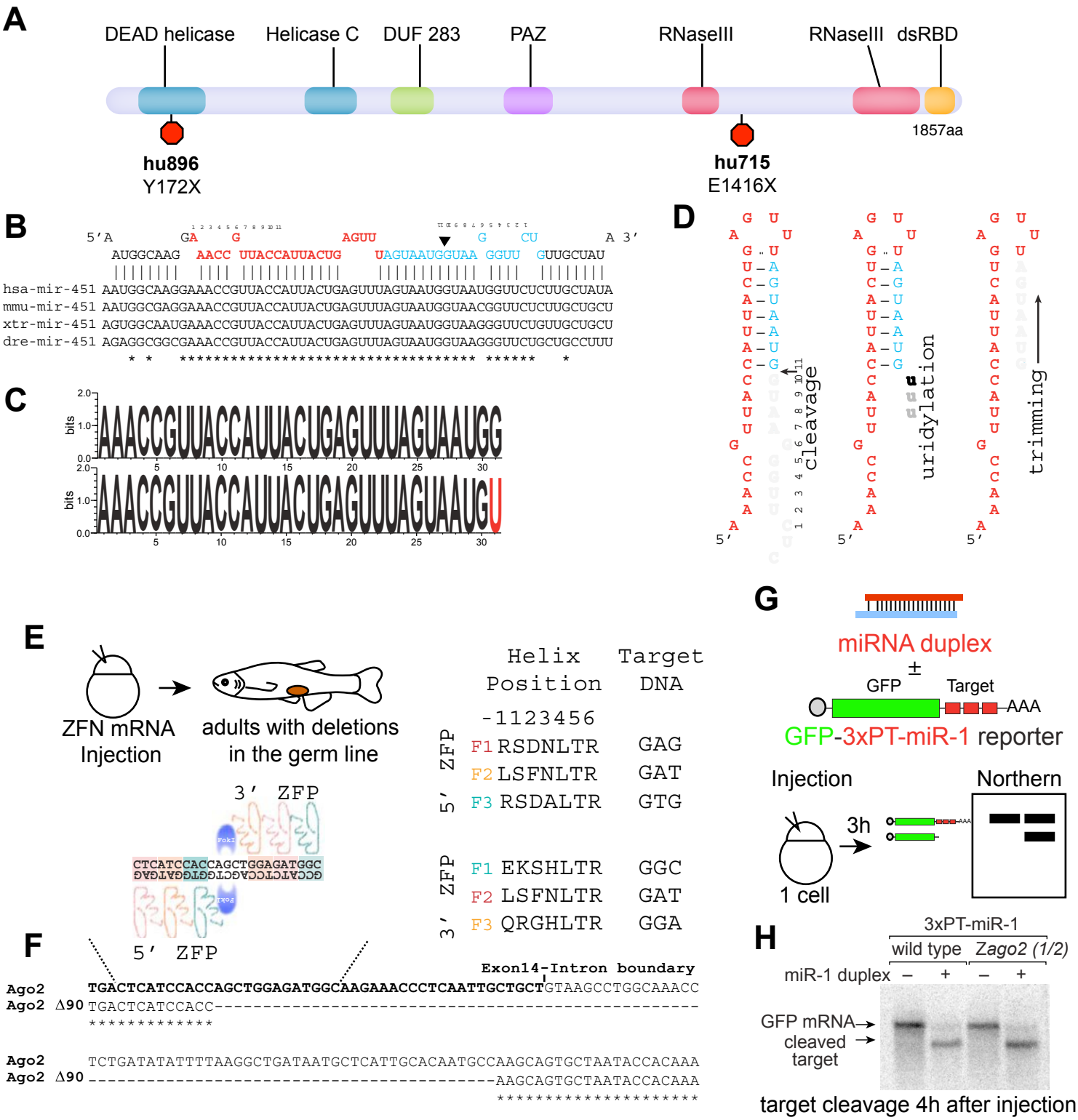

fig. S2 Cifuentes et al.

Dicer hu896						
Sample	**Reads Number**	**Filter**	**Genome**	**Genome percent**	**Pre-miR**	**Mature miR**
Dicer48h	5874173	5580719	2493924	45%	5%	4%
WT48h	12262109	12114186	2276394	19%	75%	69%

Dicer hu715						
Sample	**Reads Number**	**Filter**	**Genome**	**Genome percent**	**Pre-miR**	**Mature miR**
Dicer48h	3638005	3618442	2264413	63%	15%	9%
WT48h	1159705	1146164	871098	76%	86%	82%

Ago2 yΔ90						
Sample	**Reads Number**	**Filter**	**Genome**	**Genome percent**	**Pre-miR**	**Mature miR**
Ago48h	16915630	16901286	15900662	94%	72%	71%

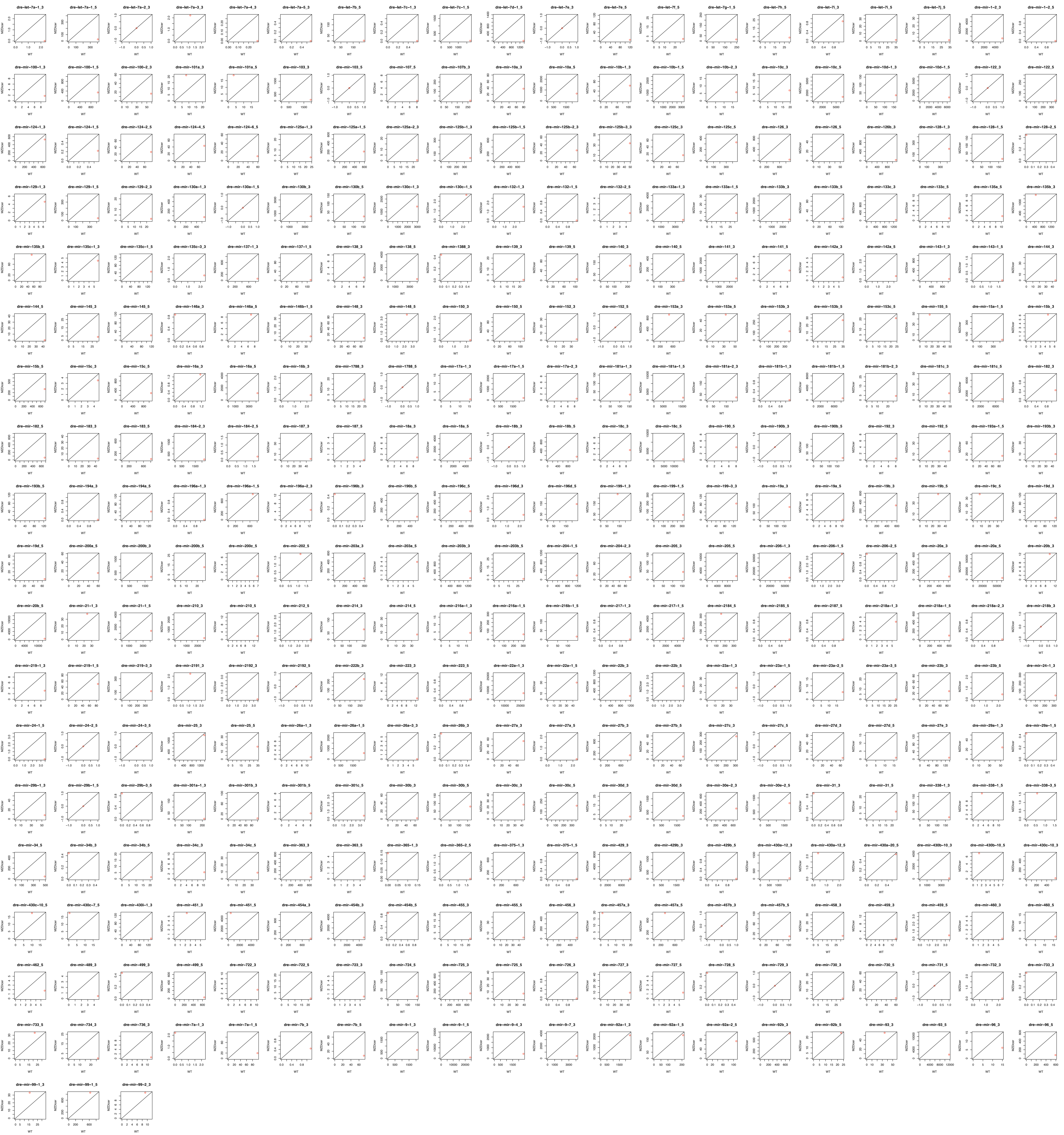

dre-let-7a-1_3
dre-let-7a-1_5
dre-let-7a-2_3
dre-let-7a-3_3
dre-let-7a-4_3
dre-let-7a-5_3
dre-let-7b_5
dre-let-7c-1_3
dre-let-7c-1_5
dre-let-7d-1_5
dre-let-7e_3
dre-let-7e_5
dre-let-7f_5
dre-let-7g-1_5
dre-let-7h_5
dre-let-7i_3
dre-let-7i_5
dre-let-7j_5
dre-mir-1-2_3
dre-mir-1-2_5
dre-mir-100-1_3
dre-mir-100-1_5
dre-mir-100-2_3
dre-mir-101a_3
dre-mir-101a_5
dre-mir-103_3
dre-mir-103_5
dre-mir-107_5
dre-mir-107b_3
dre-mir-10a_3
dre-mir-10a_5
dre-mir-10b-1_3
dre-mir-10b-1_5
dre-mir-10b-2_3
dre-mir-10c_3
dre-mir-10c_5
dre-mir-10d-1_3
dre-mir-10d-1_5
dre-mir-122_3
dre-mir-122_5
dre-mir-124-1_3
dre-mir-124-1_5
dre-mir-124-2_5
dre-mir-124-4_5
dre-mir-124-6_5
dre-mir-125a-1_3
dre-mir-125a-1_5
dre-mir-125a-2_3
dre-mir-125b-1_3
dre-mir-125b-1_5
dre-mir-125b-2_3
dre-mir-125b-3_3
dre-mir-125c_3
dre-mir-125c_5
dre-mir-126_3
dre-mir-126_5
dre-mir-126b_3
dre-mir-128-1_3
dre-mir-128-1_5
dre-mir-128-2_5
dre-mir-129-1_3
dre-mir-129-1_5
dre-mir-129-2_3
dre-mir-130a-1_3
dre-mir-130a-1_5
dre-mir-130b_3
dre-mir-130b_5
dre-mir-130c-1_3
dre-mir-130c-1_5
dre-mir-132-1_3
dre-mir-132-1_5
dre-mir-132-2_5
dre-mir-133a-1_3
dre-mir-133a-1_5
dre-mir-133b_3
dre-mir-133b_5
dre-mir-133c_3
dre-mir-133c_5
dre-mir-135a_5
dre-mir-135b_3
dre-mir-135b_5
dre-mir-135c-1_3
dre-mir-135c-1_5
dre-mir-135c-3_3
dre-mir-137-1_3
dre-mir-137-1_5
dre-mir-138_3
dre-mir-138_5
dre-mir-1388_3
dre-mir-139_3
dre-mir-139_5
dre-mir-140_3
dre-mir-140_5
dre-mir-141_3
dre-mir-141_5
dre-mir-142a_3
dre-mir-142a_5
dre-mir-143-1_3
dre-mir-143-1_5
dre-mir-144_3
dre-mir-144_5
dre-mir-145_3
dre-mir-145_5
dre-mir-146a_3
dre-mir-146a_5
dre-mir-146b-1_5
dre-mir-148_3
dre-mir-148_5
dre-mir-150_3
dre-mir-150_5
dre-mir-152_3
dre-mir-152_5
dre-mir-153a_3
dre-mir-153a_5
dre-mir-153b_3
dre-mir-153b_5
dre-mir-153c_5
dre-mir-155_5
dre-mir-15a-1_5
dre-mir-15b_3
dre-mir-15b_5
dre-mir-15c_3
dre-mir-15c_5
dre-mir-16a_3
dre-mir-16a_5
dre-mir-16b_3
dre-mir-1788_3
dre-mir-1788_5
dre-mir-17a-1_3
dre-mir-17a-1_5
dre-mir-17a-2_3
dre-mir-181a-1_3
dre-mir-181a-1_5
dre-mir-181a-2_3
dre-mir-181b-1_3
dre-mir-181b-1_5
dre-mir-181b-2_3
dre-mir-181c_3
dre-mir-181c_5
dre-mir-182_3
dre-mir-182_5
dre-mir-183_3
dre-mir-183_5
dre-mir-184-2_3
dre-mir-184-2_5
dre-mir-187_3
dre-mir-187_5
dre-mir-18a_3
dre-mir-18a_5
dre-mir-18b_3
dre-mir-18b_5
dre-mir-18c_3
dre-mir-18c_5
dre-mir-190_5
dre-mir-190b_3
dre-mir-190b_5
dre-mir-192_3
dre-mir-192_5
dre-mir-193a-1_5
dre-mir-193b_3
dre-mir-193b_5
dre-mir-194a_3
dre-mir-194a_5
dre-mir-196a-1_3
dre-mir-196a-1_5
dre-mir-196a-2_3
dre-mir-196b_3
dre-mir-196b_5
dre-mir-196c_5
dre-mir-196d_3
dre-mir-196d_5
dre-mir-199-1_3
dre-mir-199-1_5
dre-mir-199-3_3
dre-mir-19a_3
dre-mir-19a_5
dre-mir-19b_3
dre-mir-19b_5
dre-mir-19c_5
dre-mir-19d_3
dre-mir-19d_5
dre-mir-200a_5
dre-mir-200b_3
dre-mir-200b_5
dre-mir-200c_5
dre-mir-202_5
dre-mir-203a_3
dre-mir-203a_5
dre-mir-203b_3
dre-mir-203b_5
dre-mir-204-1_5
dre-mir-204-2_3
dre-mir-205_3
dre-mir-205_5
dre-mir-206-1_3
dre-mir-206-1_5
dre-mir-206-2_5
dre-mir-20a_3
dre-mir-20a_5
dre-mir-20b_3
dre-mir-20b_5
dre-mir-21-1_3
dre-mir-21-1_5
dre-mir-210_3
dre-mir-210_5
dre-mir-212_5
dre-mir-214_3
dre-mir-214_5
dre-mir-216a-1_3
dre-mir-216a-1_5
dre-mir-216b-1_5
dre-mir-217-1_3
dre-mir-217-1_5
dre-mir-2184_5
dre-mir-2185_5
dre-mir-2187_5
dre-mir-218a-1_3
dre-mir-218a-1_5
dre-mir-218a-2_3
dre-mir-218b_3
dre-mir-219-1_3
dre-mir-219-1_5
dre-mir-219-3_3
dre-mir-2191_3
dre-mir-2192_3
dre-mir-2192_5
dre-mir-222b_3
dre-mir-223_3
dre-mir-223_5
dre-mir-22a-1_3
dre-mir-22a-1_5
dre-mir-22b_3
dre-mir-22b_5
dre-mir-23a-1_3
dre-mir-23a-1_5
dre-mir-23a-2_5
dre-mir-23a-3_5
dre-mir-23b_3
dre-mir-23b_5
dre-mir-24-1_3
dre-mir-24-1_5
dre-mir-24-2_5
dre-mir-24-3_5
dre-mir-25_3
dre-mir-25_5
dre-mir-26a-1_3
dre-mir-26a-1_5
dre-mir-26a-3_3
dre-mir-26b_3
dre-mir-27a_3
dre-mir-27a_5
dre-mir-27b_3
dre-mir-27b_5
dre-mir-27c_3
dre-mir-27c_5
dre-mir-27d_3
dre-mir-27d_5
dre-mir-27e_3
dre-mir-29a-1_3
dre-mir-29a-1_5
dre-mir-29b-1_3
dre-mir-29b-1_5
dre-mir-29b-3_5
dre-mir-301a-1_3
dre-mir-301b_3
dre-mir-301b_5
dre-mir-301c_5
dre-mir-30b_3
dre-mir-30b_5
dre-mir-30c_3
dre-mir-30c_5
dre-mir-30d_3
dre-mir-30d_5
dre-mir-30e-2_3
dre-mir-30e-2_5
dre-mir-31_3
dre-mir-31_5
dre-mir-338-1_3
dre-mir-338-1_5
dre-mir-338-3_5
dre-mir-34_5
dre-mir-34b_3
dre-mir-34b_5
dre-mir-34c_3
dre-mir-34c_5
dre-mir-363_3
dre-mir-363_5
dre-mir-365-1_3
dre-mir-365-2_5
dre-mir-375-1_3
dre-mir-375-1_5
dre-mir-429_3
dre-mir-429b_3
dre-mir-429b_5
dre-mir-430a-12_3
dre-mir-430a-12_5
dre-mir-430a-20_5
dre-mir-430b-10_3
dre-mir-430b-10_5
dre-mir-430c-10_3
dre-mir-430c-10_5
dre-mir-430c-7_5
dre-mir-430i-1_3
dre-mir-451_3
dre-mir-451_5
dre-mir-454a_3
dre-mir-454b_3
dre-mir-454b_5
dre-mir-455_3
dre-mir-455_5
dre-mir-456_3
dre-mir-457a_3
dre-mir-457a_5
dre-mir-457b_3
dre-mir-457b_5
dre-mir-458_3
dre-mir-459_3
dre-mir-459_5
dre-mir-460_3
dre-mir-460_5
dre-mir-462_5
dre-mir-489_3
dre-mir-499_3
dre-mir-499_5
dre-mir-722_3
dre-mir-722_5
dre-mir-723_3
dre-mir-724_5
dre-mir-725_3
dre-mir-725_5
dre-mir-726_3
dre-mir-727_3
dre-mir-727_5
dre-mir-728_5
dre-mir-729_3
dre-mir-730_3
dre-mir-730_5
dre-mir-731_5
dre-mir-732_3
dre-mir-733_3
dre-mir-733_5
dre-mir-734_3
dre-mir-736_3
dre-mir-7a-1_3
dre-mir-7a-1_5
dre-mir-7b_3
dre-mir-7b_5
dre-mir-9-1_3
dre-mir-9-1_5
dre-mir-9-4_3
dre-mir-9-7_3
dre-mir-92a-1_3
dre-mir-92a-1_5
dre-mir-92a-2_5
dre-mir-92b_3
dre-mir-92b_5
dre-mir-93_3
dre-mir-93_5
dre-mir-96_3
dre-mir-96_5
dre-mir-99-1_3
dre-mir-99-1_5
dre-mir-99-2_3
WT
MZDicer

dre-let-7i_3
dre-mir-10c_3
dre-mir-126_3
dre-mir-133b_3
dre-mir-181a-1_5
dre-mir-18c_5
dre-mir-199-1_5
dre-mir-205_3
dre-mir-217-1_5
dre-mir-22b_5
dre-mir-27b_5
dre-mir-30d_5
dre-mir-4299_3
dre-mir-457a_3
dre-mir-725_5
dre-mir-9-1_3
dre-let-7i_3
dre-mir-10b-2_3
dre-mir-125c_5
dre-mir-133a-1_5
dre-mir-153a_3
dre-mir-140_5
dre-mir-141_3
dre-mir-152_5
dre-mir-17a-2_3
dre-mir-18b_5
dre-mir-196d_5
dre-mir-204-1_5
dre-mir-216b-1_5
dre-mir-22a-1_3
dre-mir-27a_5
dre-mir-30c_5
dre-mir-375-1_5
dre-mir-455_5
dre-mir-724_5
dre-mir-7b_3
dre-let-7h_5
dre-mir-10b-1_5
dre-mir-125c_3
dre-mir-133a-1_3
dre-mir-140_3
dre-mir-139_5
dre-mir-152_3
dre-mir-17a-1_5
dre-mir-18b_3
dre-mir-196d_3
dre-mir-203b_5
dre-mir-216b-1_5
dre-mir-22a-1_3
dre-mir-27a_3
dre-mir-30c_3
dre-mir-375-1_3
dre-mir-455_3
dre-mir-724_3
dre-mir-7a-1_5
dre-let-7g-2_3
dre-mir-10b-1_3
dre-mir-125b-3_3
dre-mir-132-2_5
dre-mir-139_3
dre-mir-150_3
dre-mir-17a-1_3
dre-mir-18a_5
dre-mir-196c_5
dre-mir-203b_3
dre-mir-216a-1_3
dre-mir-223_5
dre-mir-26b_3
dre-mir-30b_5
dre-mir-365-2_5
dre-mir-454b_5
dre-mir-723_3
dre-mir-7a-1_3
dre-let-7g-1_5
dre-mir-10a_5
dre-mir-125b-2_3
dre-mir-132-1_5
dre-mir-139_3
dre-mir-150_5
dre-mir-17a-1_3
dre-mir-18a_3
dre-mir-196c_3
dre-mir-203b_3
dre-mir-216a-1_3
dre-mir-223_3
dre-mir-26a-3_3
dre-mir-30b_3
dre-mir-365-1_3
dre-mir-454b_3
dre-mir-722_5
dre-mir-736_3
dre-mir-99-2_3
dre-let-7g-1_3
dre-mir-10a_3
dre-mir-125b-1_5
dre-mir-132-1_3
dre-mir-1388_5
dre-mir-150_3
dre-mir-1788_5
dre-mir-18a_3
dre-mir-196b_5
dre-mir-203a_5
dre-mir-214_5
dre-mir-223_3
dre-mir-26a-3_3
dre-mir-30b_3
dre-mir-301c_5
dre-mir-363_5
dre-mir-454a_5
dre-mir-722_3
dre-mir-734_3
dre-mir-99-1_5
dre-let-7f_5
dre-mir-107b_3
dre-mir-125b-1_3
dre-mir-130c-1_5
dre-mir-1388_3
dre-mir-148_5
dre-mir-1788_3
dre-mir-187_5
dre-mir-196b_3
dre-mir-203a_3
dre-mir-214_3
dre-mir-222b_3
dre-mir-26a-1_5
dre-mir-301c_5
dre-mir-363_5
dre-mir-454a_3
dre-mir-722_3
dre-mir-734_3
dre-mir-99-1_5
dre-let-7f_3
dre-mir-107_5
dre-mir-125a-2_3
dre-mir-130c-1_3
dre-mir-138_5
dre-mir-148_3
dre-mir-16b_3
dre-mir-187_3
dre-mir-196a-2_3
dre-mir-202_5
dre-mir-212_5
dre-mir-2192_5
dre-mir-26a-1_3
dre-mir-301b_5
dre-mir-363_3
dre-mir-454a_3
dre-mir-499_5
dre-mir-733_5
dre-mir-98_5
dre-mir-99-1_3
dre-let-7e_5
dre-mir-103_5
dre-mir-125a-1_5
dre-mir-130b_5
dre-mir-138_3
dre-mir-148a-1_5
dre-mir-16a_5
dre-mir-184-2_5
dre-mir-196a-1_5
dre-mir-200c_5
dre-mir-210_5
dre-mir-2192_3
dre-mir-25_5
dre-mir-301b_3
dre-mir-34c_5
dre-mir-451_5
dre-mir-499_3
dre-mir-733_3
dre-mir-98_5
dre-let-7e_3
dre-mir-103_3
dre-mir-125a-1_3
dre-mir-130b_3
dre-mir-137-1_5
dre-mir-148a_5
dre-mir-16a_3
dre-mir-184-2_3
dre-mir-196a-1_3
dre-mir-200b_5
dre-mir-210_3
dre-mir-2191_3
dre-mir-25_3
dre-mir-301a-1_3
dre-mir-34c_3
dre-mir-451_3
dre-mir-489_5
dre-mir-732_3
dre-mir-98_3
dre-let-7d-1_5
dre-mir-101a_5
dre-mir-124-4_5
dre-mir-130a-1_5
dre-mir-137-1_3
dre-mir-146a_3
dre-mir-15c_5
dre-mir-183_5
dre-mir-194a_5
dre-mir-200b_3
dre-mir-21-1_5
dre-mir-219-3_3
dre-mir-24-3_5
dre-mir-29b-3_5
dre-mir-34b_5
dre-mir-430-1_3
dre-mir-489_3
dre-mir-731_5
dre-mir-93_5
dre-let-7d-1_3
dre-mir-101a_3
dre-mir-124-4_3
dre-mir-130a-1_3
dre-mir-135c-3_3
dre-mir-145_5
dre-mir-15c_3
dre-mir-183_3
dre-mir-194a_3
dre-mir-200a_5
dre-mir-21-1_3
dre-mir-219-1_5
dre-mir-24-2_5
dre-mir-29b-1_5
dre-mir-34b_3
dre-mir-430b-7_5
dre-mir-462_5
dre-mir-730_5
dre-mir-93_3
dre-let-7c-1_5
dre-mir-100-2_3
dre-mir-124-2_5
dre-mir-129-2_3
dre-mir-135c-1_5
dre-mir-145_3
dre-mir-15b_5
dre-mir-182_5
dre-mir-193b_5
dre-mir-19d_5
dre-mir-20b_5
dre-mir-219-1_3
dre-mir-24-1_5
dre-mir-29b-1_3
dre-mir-34_5
dre-mir-430b-10_5
dre-mir-460_5
dre-mir-730_3
dre-mir-92b_5
dre-let-7c-1_3
dre-mir-100-2_3
dre-mir-124-2_3
dre-mir-129-2_3
dre-mir-135c-1_3
dre-mir-144_5
dre-mir-15b_3
dre-mir-182_3
dre-mir-193b_3
dre-mir-19d_3
dre-mir-20b_3
dre-mir-218b_3
dre-mir-24-1_3
dre-mir-29a-1_5
dre-mir-338-3_5
dre-mir-430c-10_3
dre-mir-460_3
dre-mir-729_3
dre-mir-92b_3
dre-let-7b-3_3
dre-mir-100-1_3
dre-mir-124-1_3
dre-mir-129-1_3
dre-mir-135b_5
dre-mir-144_3
dre-mir-15a-1_5
dre-mir-181c_5
dre-mir-193a-1_5
dre-mir-19c_5
dre-mir-20a_5
dre-mir-218a-2_3
dre-mir-23b_5
dre-mir-29a-1_3
dre-mir-338-1_5
dre-mir-430b-10_5
dre-mir-459_5
dre-mir-728_5
dre-mir-92a-2_5
dre-let-7b-3_5
dre-mir-100-1_5
dre-mir-124-1_5
dre-mir-129-1_5
dre-mir-135b_3
dre-mir-143-1_5
dre-mir-15a-1_3
dre-mir-181c_3
dre-mir-192_5
dre-mir-19b_5
dre-mir-20a_3
dre-mir-218a-1_5
dre-mir-23b_3
dre-mir-27a_3
dre-mir-338-1_3
dre-mir-430b-10_3
dre-mir-459_3
dre-mir-728_3
dre-mir-92a-1_5
dre-let-7b-3_3
dre-mir-11-2_3
dre-mir-122_3
dre-mir-128-1_5
dre-mir-135a_5
dre-mir-143-1_3
dre-mir-155_5
dre-mir-181b-2_3
dre-mir-192_3
dre-mir-19b_3
dre-mir-218a-1_3
dre-mir-23a-3_5
dre-mir-27d_5
dre-mir-31_5
dre-mir-430b-20_5
dre-mir-458_3
dre-mir-727_5
dre-mir-92a-1_3
dre-let-7b-2_3
dre-let-7i_5
dre-mir-104-1_5
dre-mir-125a-2_3
dre-mir-128-1_3
dre-mir-132c_5
dre-mir-142a_5
dre-mir-152c_5
dre-mir-181b-1_5
dre-mir-190b_5
dre-mir-19a_5
dre-mir-206-1_5
dre-mir-2187_5
dre-mir-23a-2_5
dre-mir-27d_3
dre-mir-31_3
dre-mir-430b-12_5
dre-mir-457b_5
dre-mir-727_3
dre-mir-9-7_3
dre-let-7a-1_5
dre-let-7i_3
dre-mir-104-1_3
dre-mir-125a-1_3
dre-mir-126_5
dre-mir-130b_3
dre-mir-137-1_5
dre-mir-141_5
dre-mir-153b_3
dre-mir-181a-2_3
dre-mir-190_5
dre-mir-199-3_3
dre-mir-200b_5
dre-mir-205_5
dre-mir-2184_5
dre-mir-23a-1_5
dre-mir-27c_5
dre-mir-30e-2_5
dre-mir-457b_3
dre-mir-9-4_3
dre-let-7a-1_3
dre-mir-10c_5
dre-mir-126_3
dre-mir-130b_5
dre-mir-137-1_3
dre-mir-141_3
dre-mir-153b_5
dre-mir-181a-2_5
dre-mir-190_3
dre-mir-199-3_5
dre-mir-200b_3
dre-mir-205_3
dre-mir-2184_3
dre-mir-23a-1_3
dre-mir-27c_3
dre-mir-30e-2_3
dre-mir-457a_5
dre-mir-728_3
dre-mir-9-1_5

fig. S5 Cifuentes et al.

Accession	ID	Stem-loop
MI0001729	hsa-mir-451	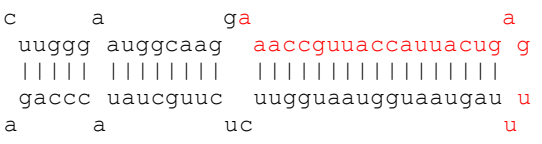
MI0001730	mmu-mir-451	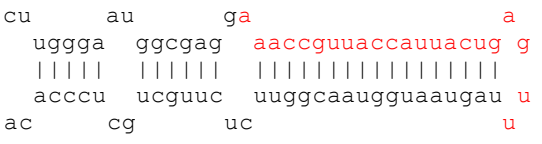
MI0001731	rno-mir-451	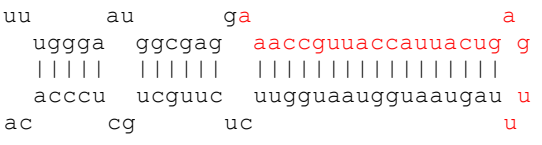
MI0001732	dre-mir-451	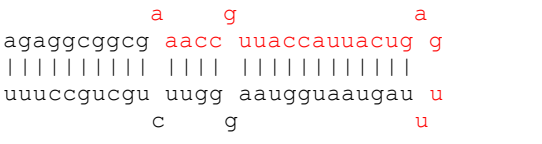
MI0004958	xtr-mir-451	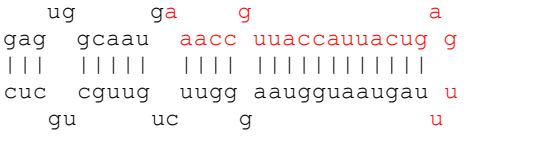
MI0004995	gga-mir-451	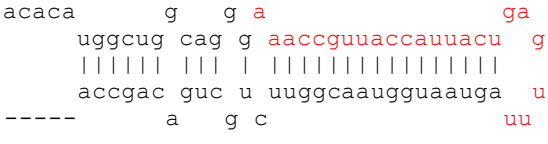
MI0005304	mdo-mir-451	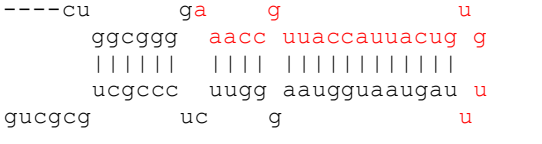
MI0006722	oan-mir-451	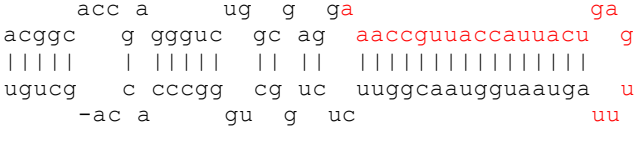
MI0007752	mml-mir-451	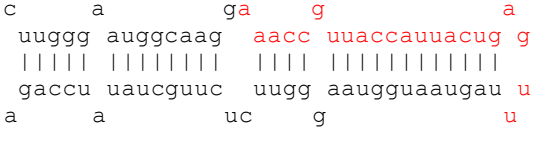
MI0008675	ptr-mir-451	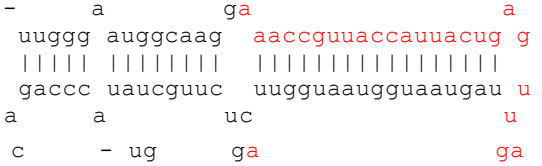
MI0009837	bta-mir-451	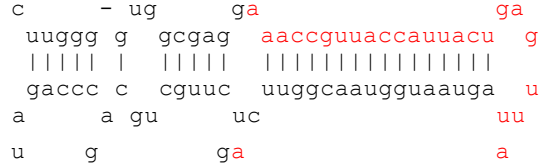
MI0010367	cfa-mir-451	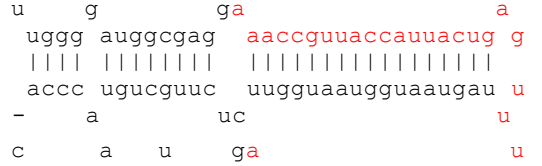
MI0012785	eca-mir-451	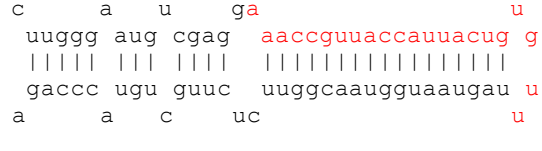

Supp Figure 6 Cifuentes et al.

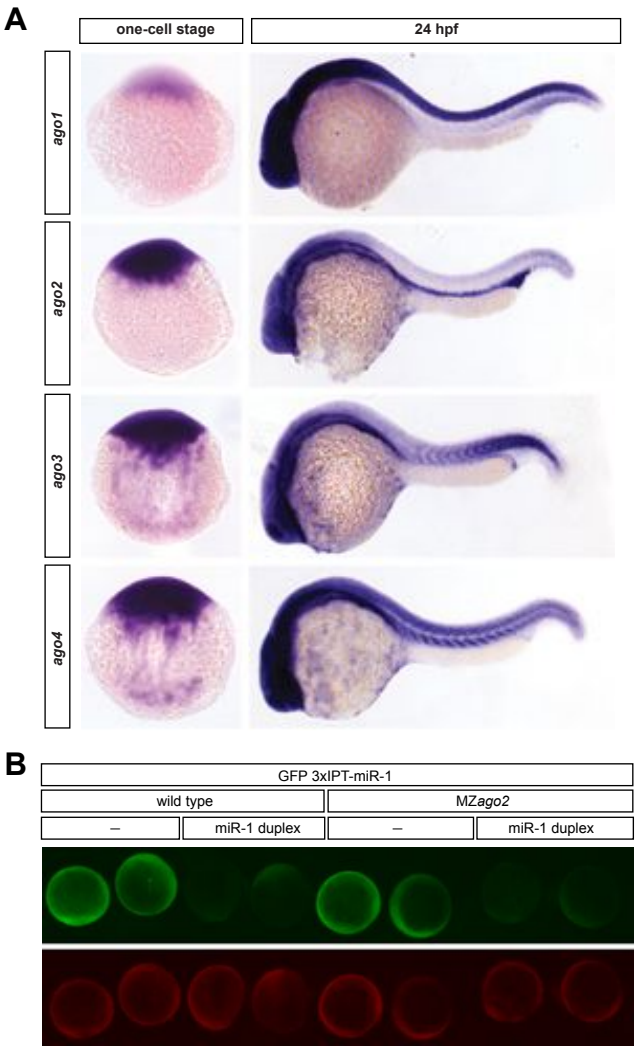

fig. S7 Cifuentes et al.

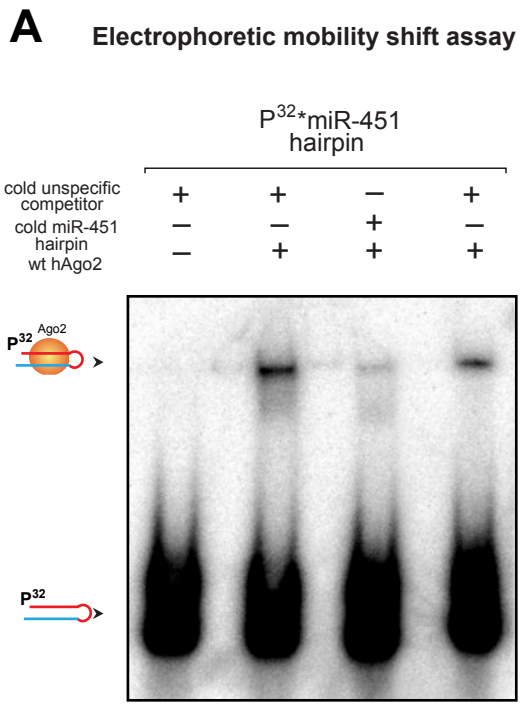

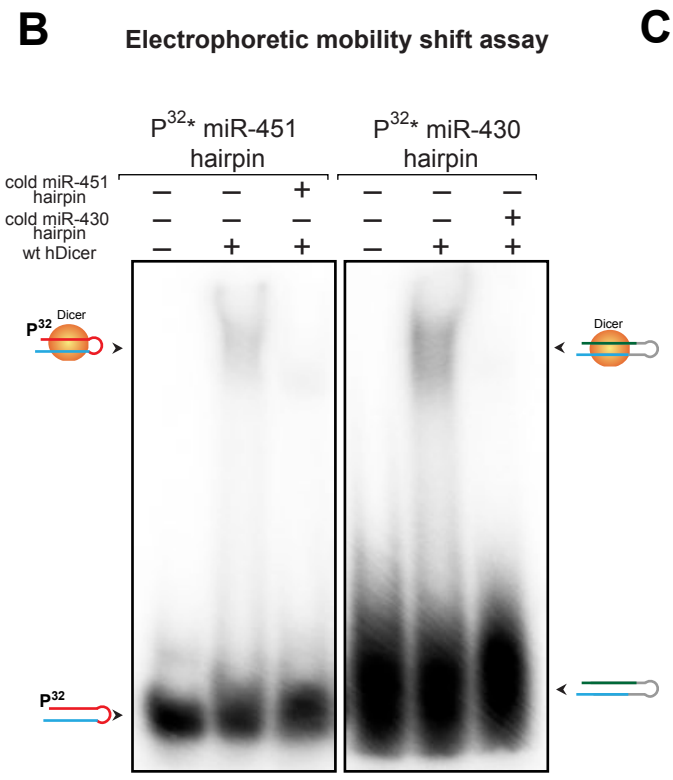

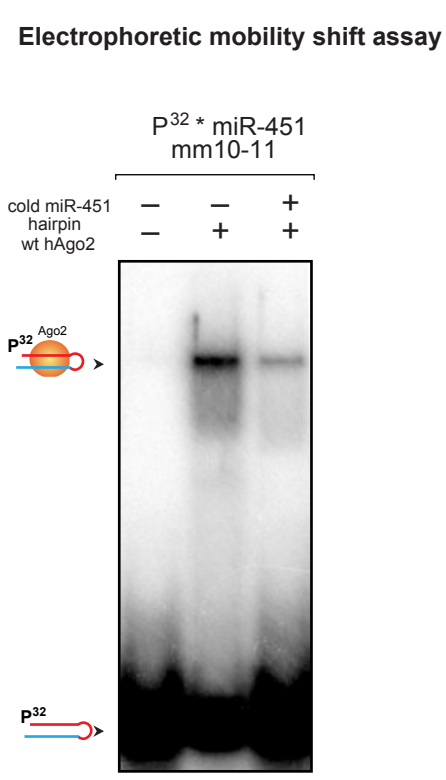

fig. S8 Cifuentes et al.

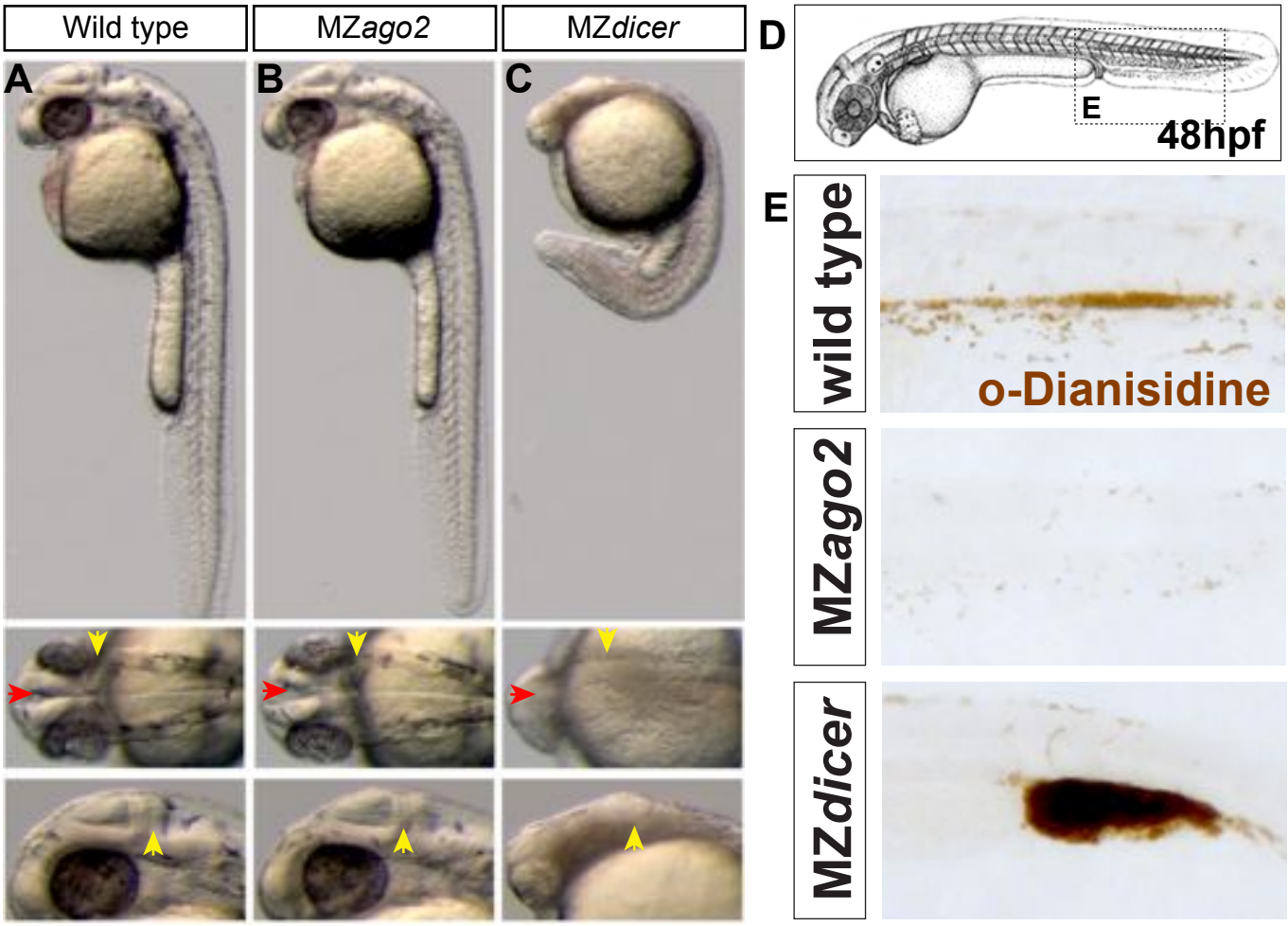

fig. S9 Cifuentes et al.

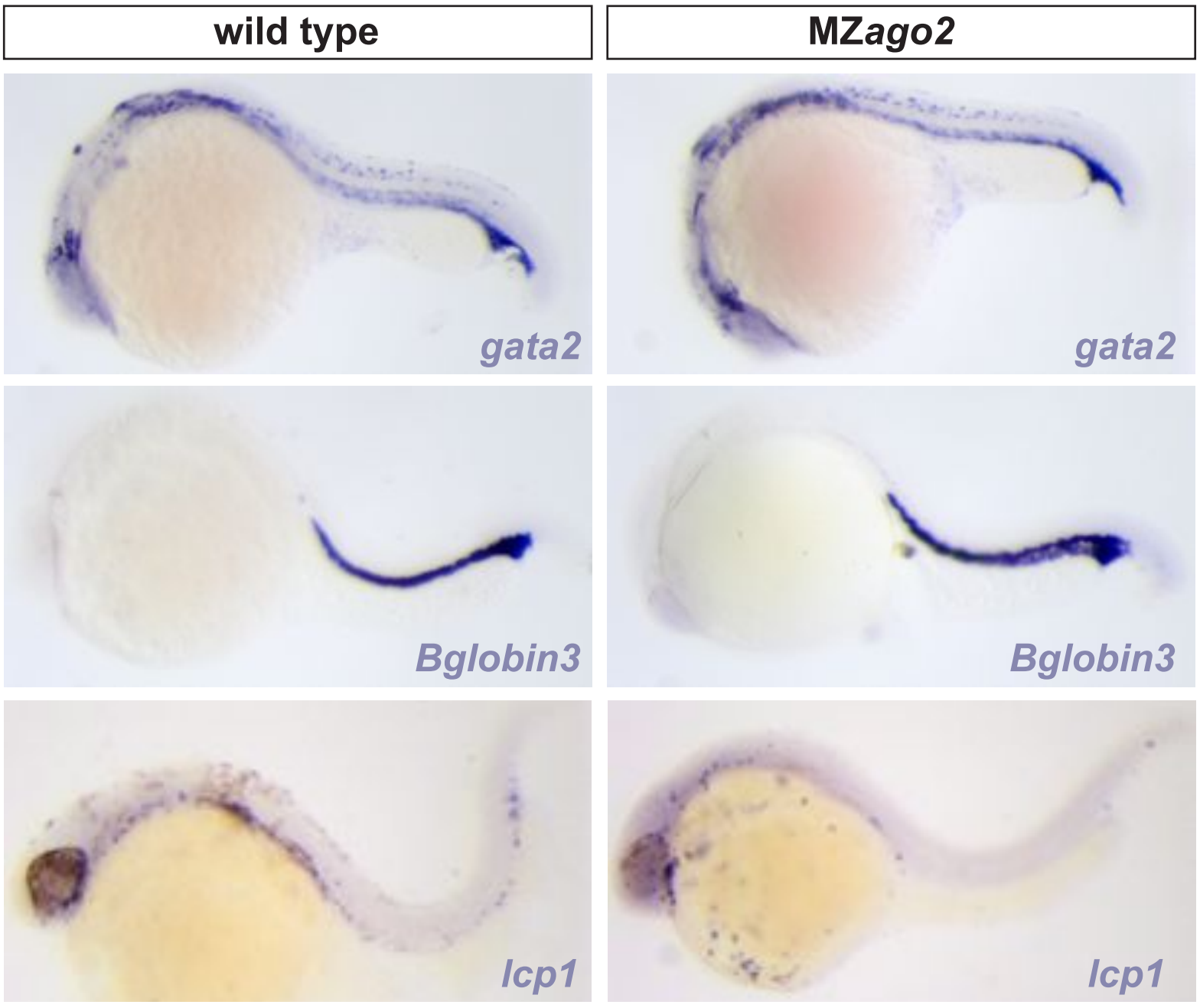

Supp Fig 10 Cifuentes et al.

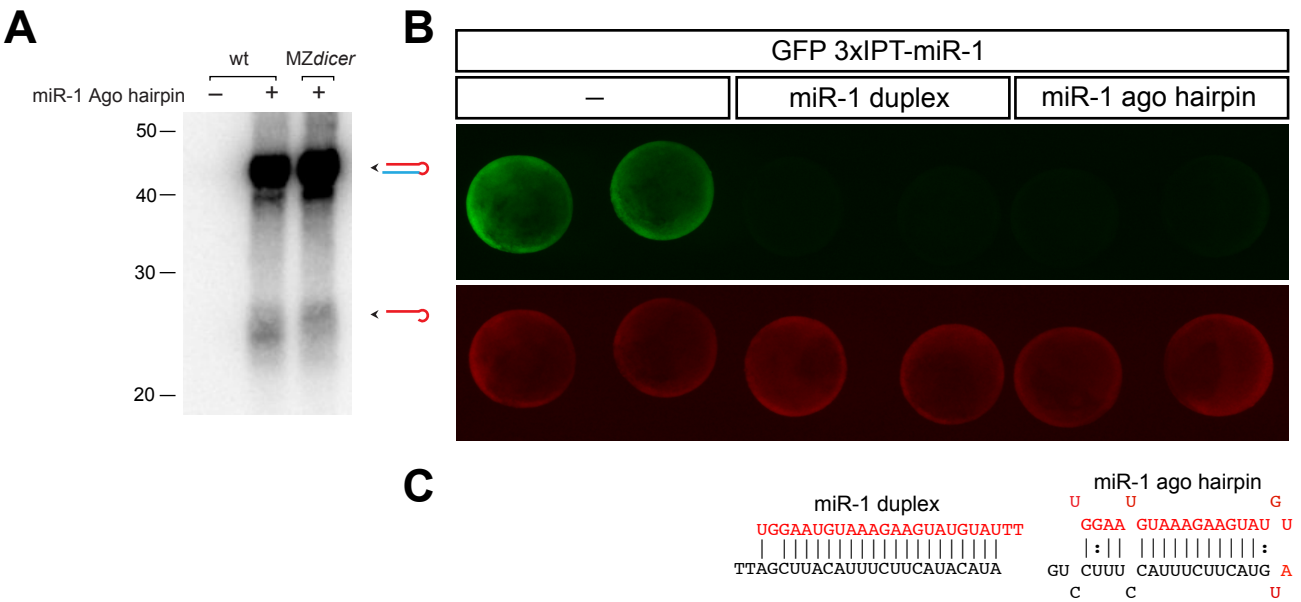

fig. S11 Cifuentes et al.